THEORETICAL ASPECTS OF FATIGUE AND CREEP CRACK GROWTH

K. Sadananda

Materials Science and Technology Division, Naval Research Laboratory, Washington, DC 20375, USA

ABSTRACT

Theoretical aspects of crack growth behavior in fatigue and creep are examined in terms of micromechanisms of growth and macromechanical considerations. Fatigue crack growth curves in terms of threshold, near-threshold, Paris-law and rapid growth regimes, and various microprocesses that affect these regimes are discussed. Threshold and near-threshold regimes are affected by both intrinsic factors such as elastic modulus, slip character, slip reversibility and microstructural heterogeneities, and extrinisic factors involving crack path tortuosity and crack closure. In the near-threshold and rapid crack growth regimes, the growth occurs by the cumulative damage processes wherein damage accumulation during several cycles is required for each increment in crack length. In the intermediate Paris-law regime growth generally occurs by the plastic blunting process. Behavior of short cracks and non-propagating cracks are discussed briefly. Crack growth in creep is discussed in terms of relative kinetics of the stress relaxation processes involving creep of the material ahead of the crack tip as well as the crack tip blunting process, and the damage accumulating processes involving void nucleation and growth and formation of microcracks ahead of the main crack. Recent developments in the parametric analysis and in the theoretical modelling of creep crack growth are briefly outlined.

KEYWORDS

Fatigue crack growth theory; stress intensity threshold; crack path tortuosity; creep crack growth; crack closure; cumulative damage; crack growth rate prediction; hysteresis.

INTRODUCTION

The early success of linear elastic fracture mechanics (LEFM) in correlating fatigue crack growth in metals has led to a number of research efforts to characterize and to understand the growth behavior in many engineering alloys. In recent years the techniques have been extended to crack growth at high temperatures where time-dependent effects such as creep and environmental effects are superimposed. In this review we discuss the

theoretical aspects of crack growth in fatigue and discuss briefly recent advances made in understanding creep crack growth.

Subcritical crack growth under cyclic or static load may be treated in terms of at least four regions, namely a) a threshold stress for crack growth, b) near-threshold crack growth, c) steady state growth and d) rapid growth to complete failure. Figure 1 shows a representative fatigue crack growth rate curve in terms of crack growth rate per cycle, da/dN, versus stress intensity range, ΔK. Somewhat similar curves have been obtained in creep. In the following we discuss extensively the fatigue crack growth behavior corresponding to the four regions and subsequently extend some of the concepts to creep crack.

FATIGUE CRACK GROWTH

Fatigue is a damage process involving irreversible plastic flow during cyclic load. The definition of damage requires a reference and the damage here is defined as that contributing to crack length increment. The process of fatigue crack growth is broadly categorized as a) cycle by cycle growth and b) cumulative damage growth where damage accumulates during several cycles before crack growth occurs. Cycle by cycle growth generally occurs by a plastic blunting process proposed by Laird (1967) to account for the formation of ductile striations on the fracture surfaces. On the other hand, void or microcrack formation ahead of the main crack, formation of secondary cracks, faceted growth of cracks and plastic tearing may all be due to a cumulative damage process. Material properties including slip reversibility, slip character such as planar or wavy slip, and microstructural heterogeneities in addition to interactive effects of load variables, temperature and environment dictate the process of crack growth. In many cases several mechanisms operate along the crack front contributing to overall growth.

For long enough cracks where LEFM is essentially valid there are limiting values of ΔK in Figure 1 corresponding to threshold stress intensity factor ΔK_{th} below which no growth occurs and K_{Ic} where overload fracture occurs. Two transition points ΔK_{T1} and ΔK_{T2} may also be defined to distinguish between the near-threshold, steady state growth, and rapid growth rate regions. The first transition ΔK_{T1} is more sharply defined for many alloy systems than the second transition. The commonly defined Paris-law regime corresponds to the steady state region. Experimental observations indicate that this regime is least sensitive to microstructure, temperature and environment as well as R, the ratio of minimum to maximum load. Threshold and near-threshold crack growth are very sensitive to microstructure and this aspect is of particular interest since it provides a means to improve fatigue resistance.

Threshold and Near-Threshold Crack Growth

Several experimental results (Suresh, 1984) indicate that crack closure effects, which are sensitive to loading parameters and environmental conditions in addition to material properties, become predominant at the near-threshold region to the extent that questions have been raised concerning the existence of a true threshold as a material property. Furthermore, the observed growth of short cracks below the threshold for long cracks raises additional doubts about the existence.

In this paper we presume that there is a true or intrinsic threshold which depends on the micromechanism of crack growth and superimposed on this are

effects due to crack path tortuosity, residual stresses due to prior crack tip plasticity and environmental reactions at and behind the crack tip. That a threshold exists even in an inert environment at high R ratios where crack closure effects are not present is an indication that there is an intrinsic threshold characteristic of a material. Formally we can represent ΔK_{th} as

$$\Delta K_{th} = \Delta K_{th}^{(i)} + \Delta K_{th}^{(e)} \qquad (1)$$

where superscripts i and e corresponds to intrinsic and extrinsic factors contributing to the observed threshold.

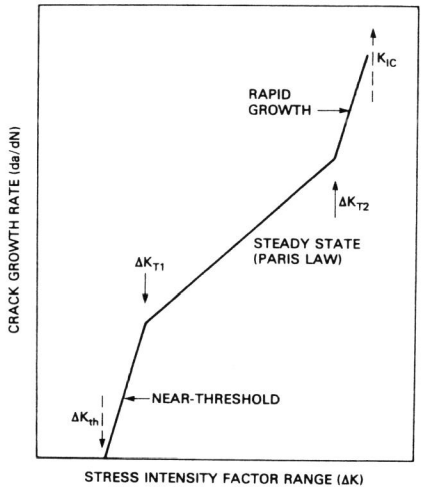

Fig. 1. A representative fatigue crack growth behavior in metals and alloys.

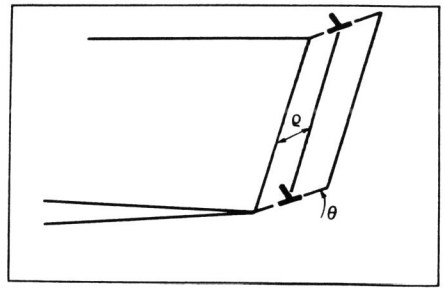

Fig. 2. Schematic illustration showing dislocation nucleation from the crack tip

Intrinsic Threshold

Since plastic flow during cycling is fundamental to the fatigue process and plasticity is associated with the nucleation and motion of dislocations, it is apparent that the threshold for crack growth is equal to or greater than the stress necessary for the generation of dislocations from the crack tip. Dislocation generation from the crack tip and its relevance to threshold has been addressed by several authors. For example, Sadananda and Shahinian (1977) have represented the threshold stress intensity for dislocation generation as

$$K_{th} = \frac{\sqrt{2\pi b}}{A}\left(\frac{\mu}{4\pi(1-\nu)} \ln \frac{\alpha\rho}{b} + \frac{\mu b}{4\pi(1-\nu)\rho} + \frac{\gamma}{\sqrt{2}\, b} + \frac{\sigma}{2}\right) \qquad (2)$$

where the four terms on the right hand side respectively are contributions from self energy of the dislocation, image force, surface energy of the ledge formed and the friction stress which is taken to be the yield stress

of the material. Here μ is the shear modulus, ρ is the dislocation distance from the crack tip, α is dislocation core constant, b is the Burgers vector, ν is the Poisson's ratio and A is the orientation factor of the slip plane with respect to crack plane and is equal to $\sin(\theta/2)\cos^2(\theta/2)$ where angle θ is shown in Fig. 2. A schematic illustration of the process is shown in Fig. 2. The first and the second terms are the predominant terms which are proportional to the elastic modulus. In fact it was shown that the intrinsic threshold normalized in terms of elastic modulus is nearly constant for several metals and alloys. Yokobori and others (1975) have also deduced a somewhat similar formulation for an intrinsic threshold.

While the above analysis is based on energetics, Weertman (1981) analyzed recently the crack tip blunting process extending the BCS type of analysis very close to the crack tip. The threshold for common metals and alloys can be represented in terms of the stress intensity necessary for blunting as

$$K_{th} = \frac{0.34}{A}\sqrt{\frac{2\mu\gamma}{(1-\nu)}} \qquad (3)$$

and to insure blunting instead of rapid growth of a crack by cleavage the above stress should be less than the Griffith stress given by

$$K_{IG} = \frac{1}{A}\sqrt{\frac{2\mu\gamma}{(1-\nu)}} \qquad (4)$$

thus eq. (4) represents an upper bound for a true threshold. In reality eqs. (3) and (4) are valid for a virgin crack with no prior plastic blunting of the crack tip. Experimentally thresholds are usually determined by load shedding techniques where conditions for the arrest of a growing fatigue crack are determined. Therefore an intrinsic threshold value could be greater than the Griffith's stress since the cleavage process has already been circumvented due to prior fatigue damage. A simple calculation for Fe using $\mu=7\times10^{11}$ dynes/cm^2, γ = 1900 ergs/cm^2 and $\cos(\theta)$ = 1/3 gives K_{th} = 0.65 MPa$\sqrt{m}$ and K_{IG} = 1.9 MPa$\sqrt{m}$. Implication of the analysis is that crack tip blunting occurs at very low stress intensities much less than the observed threshold values. It is important to recognize at this point that experimental threshold stress intensities are usually defined as that corresponding to crack growth rates less than 10^{-10} to 10^{-11} cm/cycle, crack length increments per cycle much less than the interatomic spacing. On the other hand, the dislocation nucleation process that results in crack tip blunting and crack growth provides minimum growth rates very close to the interatomic spacings.

To explain lower crack growth rates, one could consider the orientation effects in a polycrystalline material. The orientation of the crack plane in each grain changes due to changes in the orientation of the slip planes although the average orientation may still be normal to the stress axis. Even if a crack length increment occurs by a Burgers vector distance in each grain, the average nominal crack length increment could be less than the interatomic distance by a factor of m where m is the average orientation factor. For a randomly oriented polycrystal, m may vary between two to three (Taylor, 1938) and growth per cycle may not be less than a factor of two to three Burgers vector. Actually, the change of the crack plane from grain to grain affects, in addition to crack growth increment per cycle, the effective stress intensity due to the tortuous crack path. Effects of crack path tortuosity will be discussed later.

Since crack growth rates are usually less than 10^{-9} cm/cycle in the

near-threshold regime, then near-threshold crack growth occurs more likely by a cumulative damage process with damage accumulating in each cycle until some critical event occurs contributing to a discrete increment in crack length. Crack growth rates can be much less than 10^{-9} cm/cycle if for each small increment in crack length, damage accumulation during many cycles is required. Figure 3 shows types of damage that can occur locally ahead of the crack tip contributing to a discrete increment in crack length. At low temperatures a faceted mode of crack growth was frequently observed in high strength planar slip materials with facets parallel to slip plane, cleavage plane, and, in some cases, grain boundaries or two-phase interfaces (Gell and Leverant, 1968; Yoder, Cooley and Crooker, 1977; Sadananda and Shahinian, 1981; Gerberich and Moody, 1979). One can distinguish between two types of faceted growth purely based on fractographic evidence. Large transgranular facets of the order of grain size and grain boundary facets that show river lines characteristic of conventional cleavage fracture are one type. Each facet is formed in one burst by stress concentrations produced in the neighboring grains. These become more predominant in the final rapid growth stage, Fig. 1. The second type of facet formation results somewhat progressively with each burst producing a part of the total facet. This leaves markers on the fracture surface corresponding to each crack length increment and are called brittle striations to distinguish them from ductile striations formed by the plastic blunting process.

What constitutes the threshold in this case is difficult to assess since it will depend on the mechanism of growth. While the dislocation nucleation at the crack tip may be a necessary event for accumulation of damage, the growth is ensured only when the local fracture event can occur. To a first approximation it can be reasonably assumed that cyclic strain may be accumulated if stresses ahead of the crack tip are greater than the cyclic yield stress of the material. If the fracture size is related to the dislocation cell size d as appears to be the case, indicated by several observations (Mughrabi, Herz and Stark, 1981; Davidson, 1979), then the threshold stress can be represented by

$$\Delta K_{th}^{(i)} = m\,\sigma_{cy}\sqrt{2\pi d} \qquad (5)$$

where m is the average orientation factor which for a polycrystal may be between two and three. The grain size dependence of the threshold depends on the variation of σ_{cy} and d with grain size. Lucas and Gerberich (1983) analyzed this somewhat differently considering the reversed plastic zone produced during cycling and deduced an expression for threshold. Starke and others (1984) provided recently an alternate analysis based on the Chakaraborty (1979) model of fatigue crack growth. It is, however, difficult to compare the predictions of each model since several of the material parameters required for computation are unknown. We may also mention here than Lin and Fine (1982) suggested a somewhat similar relation to eq. (5) for intrinsic threshold where stress corresponds to the stress required to activate a dislocation source at a distance d for the crack tip. If the source is identified by the dislocation cell wall then the strength of the source is $\sigma_s = \mu b/d$ where d is the cell size. Eq. (5) can be represented as

$$\Delta K_{th} = m\,\mu b\sqrt{\frac{2\pi}{d}} \qquad (6)$$

Both equations (5) and (6) assume that strain accumulation continues until a local fracture event occurs. Crack growth rates near the threshold, however,

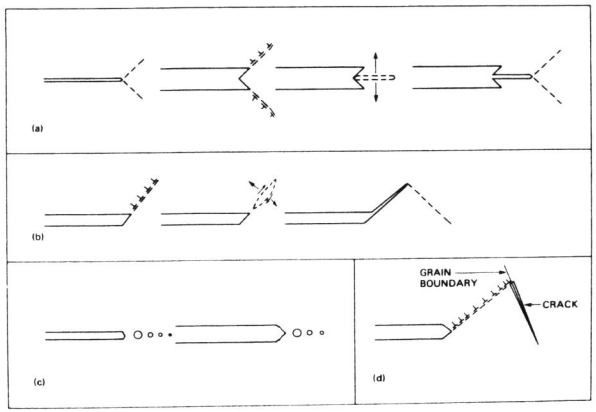

Fig. 3. Cumulative damage processes that can occur ahead of the crack tip contributing to crack growth. a) Faceted growth along a cleavage plane, b) faceted growth along a slip plane, c) void nucleation and growth, and d) crack nucleation along high energy interface (grain boundary, sub-boundary, two-phase interface, etc.).

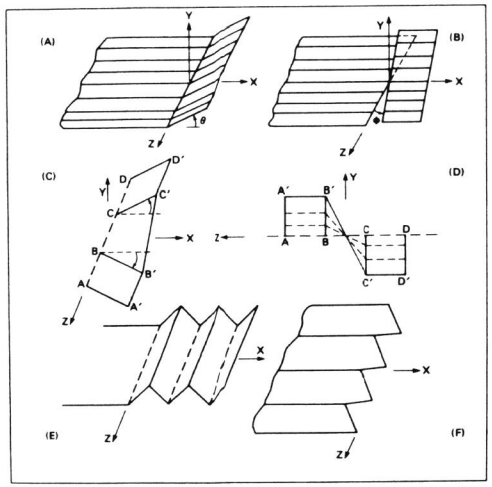

Fig. 4. Schematic illustration of Mode I crack deflection during its growth a) tilt of angle θ, b) twist of angle ϕ, c) combined tilt and twist deflections - segment AB and CD tilt in two opposite directions. Segment BC undergoes continuous twist to maintain continuity, d) projection of figure c on Y-Z plane, e) zig-zag tilt along X-direction, and f) zig-zag crack front along Z-direction.

depend on the number of cycles required to accumulate the critical strain to cause the fracture of the ligament equivalent to the dislocation cell size. We will address next the factors governing the extrinsic threshold.

Extrinsic Threshold

Extrinsic factors that contribute to the threshold value as well as crack growth rates include crack path tortuosity and crack closure effects arising from several sources. The distinction between the intrinsic and extrinsic factors is somewhat arbitrary since for example crack path tortuosity is in fact related to the intrinsic mechanisms of crack growth. Since it is a geometric effect induced by fluctuations in the crack path we consider it an extrinsic factor. Similarly some of the factors that contribute to crack closure effects are also related to the mechanisms of crack growth. Either by the plastic blunting process or by the cumulative damage process involving faceted mode of crack growth, crack path becomes tortuous particularly at the near-threshold crack growth regime and its effects therefore are important. This aspect is therefore discussed in detail.

Crack path tortuosity and its effect on crack growth rates. The crack plane orientation changes both along the crack growth direction as well as along the crack front due to variations in the orientations of the slip planes in each grain as well as due to local variations in the microstructure such as precipitates, interfaces etc. Because of these, crack deflections occur contributing to tilt and twist segments involving combined Modes I and II or I and III although the average growth may still be Mode I. These deflections reduce the effective stress intensity factor in addition to increasing crack surface area per unit increment in the crack length. Effects of simple tilt deflections in two dimensional crack path tortuosity involving both tilt and twist components are discussed.

Figure 4 (a and b) shows the geometry of Mode I crack deflected contributions to tilt and twist components. If the nominal growth is Mode I, a continuous tilt or twist (a tilt along the crack front) can result as shown in Fig. 4 e and f. In reality, however, both tilt and twist segments may be present along the crack front. In fact twist components arise when two neighboring segments along the crack front tilt in opposite directions. Fig. 4 c and d shows two views of the crack front as it tilts and twists to maintain continuity during its growth. Even if the tilt angle θ is constant in Fig. 4c, the twist angle ϕ increases from zero to a maximum as the segment BC grows to B′C′. Analysis of this problem is more complex and for simplicity we assume constant tilt and twist angles along the crack front.

Figure 5 shows an idealization of the crack front configuration as it tilts and twists. Crack front is represented in terms of a zig-zag path along the boundaries of a regular hexagon. Projection along the crack front (Z direction) is shown in Fig. 5a. The configuration is similar to that considered by Faber and Evans (1983). From the geometry the fractions of the tilt and twist segments are given by

$$t_f = \frac{\sin(\phi)}{\sin(\phi)+\cot(\phi)} \qquad (7a)$$

and

$$T_f = \frac{\cot(\phi)}{\sin(\phi)+\cot(\phi)} \qquad (7b)$$

Looking along the crack front, tilt does not increase the crack front length

while twist does and the fractional change in length is given by cos(ϕ). The total average effective K due to tilt and twist along the crack front is represented by

$$K_{eff} = t_f K_t + T_f \cos(\phi) K_T \quad (8)$$

where K_t and K_T are stress intensity contributions from tilt and twist cracks. K_t components are readily available in the literature and are discussed by Suresh (1983). In particular they are represented by

$$K_t = K_I \sqrt{(a_{11}^2 + a_{21}^2)} \quad (9)$$

where K_I is the Mode I stress intensity factor of an undeflected crack and a_{11} and a_{21} are trigonometric functions representing the normal and shear stress components on the deflected plane, Fig. 4a. These are given by $a_{11} = \cos^3(\theta/2)$ and $a_{21} = \sin(\theta/2)\cos^2(\theta/2)$.

The twist components for Mode I crack are not readily available in the literature but from simple coordinate transformation shown in Fig. 4b and using stress components ahead of a Mode I crack we deduce the normal and tangential stress contributions for a twisted crack as

$$K^1_T = A_{11}K_I = K_I \cos(\theta/2)\,[\cos^2(\phi)\,\{1+\sin(\theta/2)\sin(3\theta/2)\} + 2\,\nu\,\sin^2(\phi)]$$

$$K^3_T = A_{31}\,K_I = -K_I \cos(\phi)\,\sin(\phi)\,[\cos(\theta/2)\{(2\nu-1)-\sin(\theta/2)\sin(\theta/2)\}] \quad (10)$$

We note that Faber and Evans (1983) deduced somewhat different expressions for twist segments where they considered twist of a crack which has already been tilted by angle θ. The effective stress intensity due to twist of Mode I crack is then given by

$$K_T = K_I \sqrt{(A_{11}^2 + A_{31}^2)} \quad (11)$$

Using eq. 8 an effective stress intensity due to tilt and twist along a crack front can be determined. Such a crack front, Fig. 5a, undergoes further deflections as it grows along the X-direction indicated by Fig. 5b where D and S segments correspond to deflected and straight segments along the X-axis. If viewed normal to the crack front, there are both tilt and twist segments along the deflected segment D and only alternate straight and twist segments along S. The average effective stress intensity factor for crack with D and S segments is given by

$$K_{eff} = \frac{[D\,\{t_f K_I + T_f \cos(\phi)\,K_T\} + S\,\{t_f K_I + T_f \cos(\phi)\,K_T\}]}{(D+S)} \quad (12)$$

For equiaxed grains, D = S and the effective stress intensity is given by

$$K_{eff} = K_I \left[\frac{t_f\,(3+\cos(\theta))}{4} + T_f \cos(\phi)\,(A_{11}^2 + A_{31}^2)^{0.5}\right]$$

$$= K_I\, F(\theta,\phi) \quad (13)$$

For cyclic load K in eq. 13 are to be replaced by ΔK. The actual stress

intensity ahead of the tortuous crack tip is much less than the applied stress intensity deduced on the basis of undeflected Mode I crack. If it is assumed that crack growth is dictated by the strain energy release rate, then to compensate for the reduced stress intensity, the applied stress intensity has to be increased proportionately to obtain the same growth rates. Effectively these deflections increase the crack growth resistance.

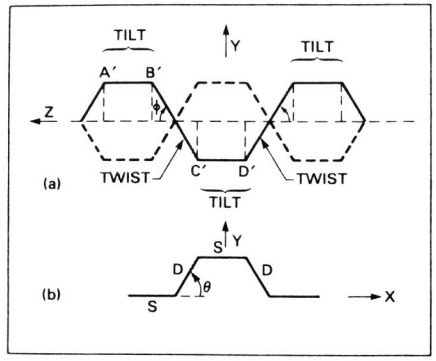

Fig. 5. a) Idealization of crack front undergoing tilt and twist deflections. A′ B′, C′ D′ are projections of tilt segments and B′ C′ the twist segment in between, b) further deflection of the crack front along the growth direction with D=S.

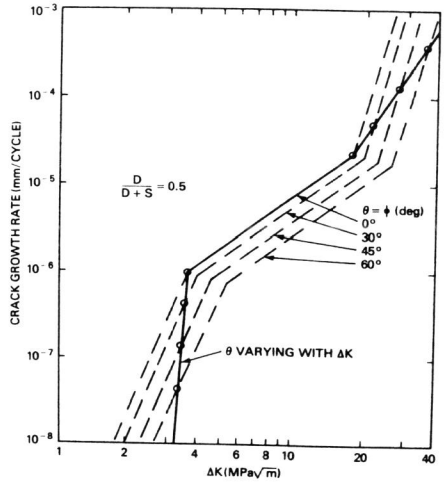

Fig. 6. Effect of crack deflection on the crack growth rate curve. Increase of θ and ϕ shifts the curves to the right.

In addition to lowering the effective stress intensity, crack deflections also increase crack length. The effect of crack length increase along the crack front has already been considered in the determination of K_{eff}. There is an increase of crack surface due to deflections along the growth direction. The weighted average growth rate represented in terms of nominal Mode I growth rate is given by

$$\frac{da}{dN}_{eff} = \frac{D\cos(\theta)+S}{D+S}\,\frac{da}{dN} \quad (14)$$

where da/dN represents the growth rate of an undeflected crack. For the case of D=S,

$$\frac{da}{dN}_{eff} = \cos^2(\theta/2)\,\frac{da}{dN} \quad (15)$$

implying that for the same ΔK_{eff} the growth rate for a deflected crack is always less than for an undeflected crack. For the case of D=S and θ=ϕ, the effect of crack path tortuosity on da/dN-ΔK relations is determined for

various selected values of θ and φ and the data are represented in Fig. 6. For a 60° deflection the stress intensity is increased by a factor of 1.5 as compared to an increase of 1.14 for simple deflection along the growth direction observed by Suresh (1983). In addition, in both cases there is a decrease in growth rates by a factor of 0.75. Thus crack path tortuosity has a significant effect on da/dN-ΔK curves.

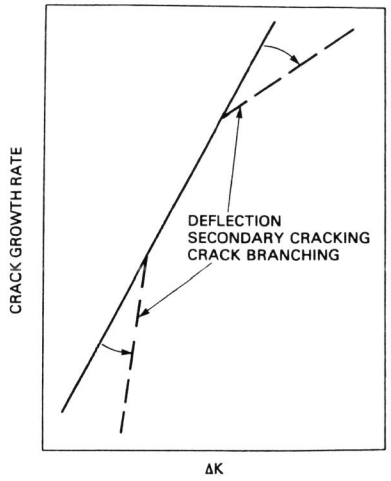

Fig. 7. Effect of crack deflection, secondary cracking and crack tip branching on the shape of crack growth rate curve.

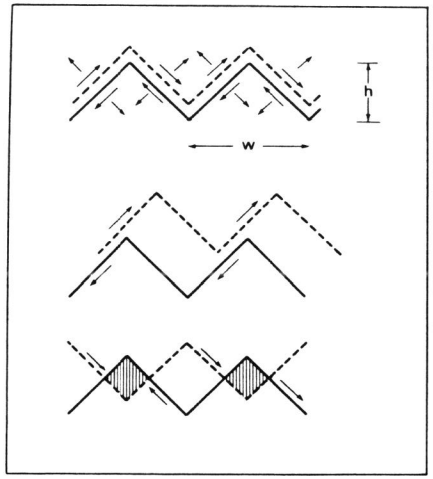

Fig. 8. Crack closure due to sliding displacements (Mode II). Rigid displacements are shown to indicate the contact of the matting surfaces due to sliding.

A constant angle of deflection is an idealization of the actual crack growth process. The angle could be a function of grain size, slip character and microstructural heterogeneities that could determine the local fracture process. With increase in ΔK the plastic zone size increases and when it is larger than the average grain size then the crack propagation mechanism could change from a faceted mode to a plastic blunting process. The angle of deflection may decrease with increase in ΔK. Thus if θ is large close to the threshold and if it decreases with increase in ΔK, then crack growth rate shifts from one curve to the next in Fig. 6 giving a much steeper da/dN-ΔK curve at the near threshold regime. On the other hand at the higher ΔK regime where monotonic fracture processes are superimposed to an increasing extent with an increase in ΔK, θ increases with ΔK and this has the effect of decreasing the da/dN-ΔK slope. Effect of crack deflection on crack growth rate curve is schemetically shown in Fig. 7. Crack tip branching and secondary cracking also reduce the effective ΔK at the crack tip and their effects on crack growth rate are similar to the crack path tortuosity. We will next consider another important extrinsic factor, namely crack closure which can contribute to the reduction of the effective stress intensity factor range.

Crack closure effects. Premature closure of the crack surfaces way behind the crack tip reduce the effective stress intensity amplitude at the crack tip. Important contributions to premature closure are surface roughness produced due to crack path tortuosity, residual stresses due to prior plastic zone at the the crack tip and oxidation products that form on the freshly created fracture surfaces. The total closure stress intensity can be represented by

$$K_{cl} = K_{cl}^{S} + K_{cl}^{R} + K_{cl}^{O} \qquad (16)$$

where the terms on the right side respectively are contributions due to surface roughness, residual stresses and oxidation products.

The roughness induced closure arises due to Mode II component arising from crack deflections. Figure 8 shows a zig-zag crack profile created due to continuous crack deflections. The sliding contributions due to Mode II component can bring the asparities to overlap each other to the extent that crack surfaces meet each other before complete unloading. Further unloading would only apply compressive stresses at the contact surfaces reducing the effective stress intensity range. From Fig. 8 the closure level can be estimated assuming that contact occurs when the normal displacements due to Mode I just balances the sliding displacement produced due to Mode II. This is given by

$$\frac{K_{cl}^{S}}{K_{max}} = \frac{K_{t}^{II}}{2K_{t}^{I}} = \frac{\cos^2(\theta/2)\,\sin(\theta/2)}{2\cos^3(\theta/2)} = \frac{1}{2}\tan(\theta/2) = \frac{h}{2W} \qquad (17)$$

where K_t^I and K_t^{II} are Mode I and Mode II components of the stress intensity factor for crack deflection with an angle θ. For θ-60°, closure level is 0.29 times K_{max}. To compensate for this reduction in the stress intensity amplitude, the applied stress intensity needs to be increased proportionately to maintain the same growth rate. If h/2W is considered as a measure of the degree of surface roughness, it can be large at low ΔK close to threshold and decrease with increase in ΔK. Note that this contribution is over and above the reduction of the effective stress intensity due to crack path tortuosity discussed earlier. In fact the closure effects are present only during cyclic load whereas the reduction due to crack path tortuosity exists even during monotonic loading. Since roughness induced crack closure is essentially due to crack path tortuosity, all of the material parameters that affect the tortuosity also affect the closure contribution.

As the crack tip moves forward, a zone of plastic region is left behind which can exert compressive stresses on the crack surfaces contributing to premature crack closure. Elber's original model (1928) of crack closure pertains to only this contribution although his experimental data may contain other contributions as well. This plasticity induced crack closure has been analyzed by a number of authors and we discuss here a simplified dislocation model treated by Kanninen and Atkinson (1980). Figure 9 shows that the plastic zone is represented by a superdislocation of Burgers vector B at a distance L from the crack tip. Elastic displacements at the crack surfaces due to the presence of dislocations are of compressive type and at the closure stress, displacements due to the superdislocation are balanced

by the elastic displacements. The closure stress intensity is then given by

$$K_{cl}^{R} = \left(\frac{9}{8\pi}\right)^{0.5} \frac{EB}{\sqrt{L}} \sin(\theta)\cos(\theta/2) \qquad (18)$$

where E is the Young's modulus and θ is the slip plane angle. From Rice's analysis (1974) the plastic zone is given by

$$R = 0.155\ (K_{max}/\sigma_y)^2 \qquad (19)$$

and the crack tip displacement is given by

$$\delta = 0.5\ K^2/(\sigma_y E) \qquad (20)$$

The Burger's vector of the superdislocation B is equal to δ/2 and the position of the dislocation L is approximately equal to R/4 corresponding to a center of gravity of a pile up. Substitution of these values in eq. 18 provides an expression for K_{cl}^{R} and is given for cos(θ) = 1/3 by

$$\frac{K_{cl}^{R}}{K_{max}} = 0.575 \qquad (21)$$

The superdislocation model provides an over estimation of the closure effect since the dislocation strength is actually smeared along the plastic zone. If reversed plastic zone is also considered and is subtracted from the effect of the monotonic plastic zone a more realistic value can be obtained. This may be estimated by considering another superdislocation with negative Burger's vector of the strength and position given by the cyclic crack tip opening displacement and cyclic plastic zone size. This together with eq. 21 is given by

$$K_{cl}^{R} = 0.575\ K_{max} - 0.28\ \Delta K = K_{max}\ (0.3 + 0.28\ R) \qquad (22)$$

Elber [19] showed that experimental data for an aluminum alloy fits the relation

$$K_{cl} = (0.5 + 0.1R + 0.4R^2)\ K_{max} \qquad (23)$$

But as pointed out earlier this could include closure contributions from other sources such as surface roughness and oxide layer. The contribution from the oxide formation can be significant at near-threshold growth rates because very low crack growth rates result in sufficiently long times for the reactions to occur behind the crack tip. Closure occurs because the volume of the oxidation products are generally larger than that of the reactants [2]. Volume expansion brings the fracture surfaces closer contributing to premature closure during unloading.

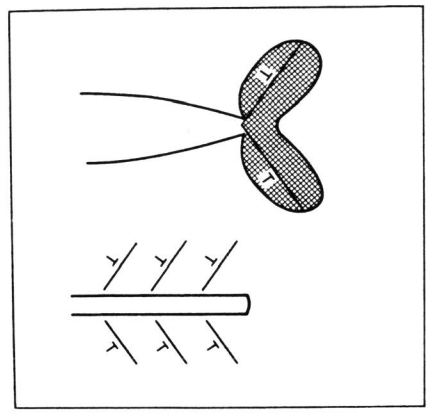

Fig. 9. a) Superdislocation approximation of crack tip plasticity, b) dislocation representation of plastic strain field behind the crack tip.

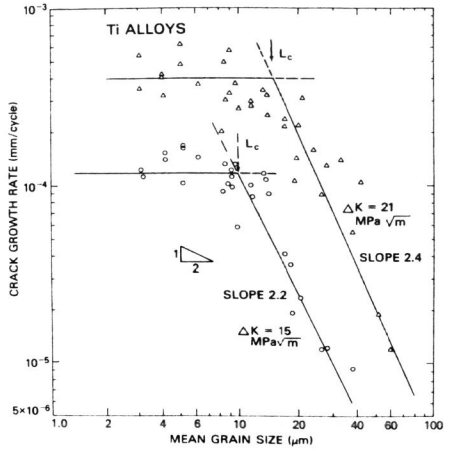

Fig. 10. Effect of grain size on crack growth rate in Ti alloys.

Both closure effects as well as the crack path tortuosity reduce the effective stress intensity at the crack tip. If the driving force for the crack growth is related to energy release rate then to compensate for the reduced effective stress intensity, the applied stress intensity needs to be increased proportionately. Determination of the intrinsic ΔK is difficult since it involves the knowledge of all of the extrinsic factors including crack path tortuosity effects and closure effects. Errors in the closure measurements can be significant, particularly in the near-threshold regime to the extent that questions have been raised conerning the utility and significance of the experimental measurements of thresholds as material property. There appears to be increasing consensus that the extrinsic factors depend on particular environment and loading conditions that it becomes important to consider the actual service environments and loading conditions to determine the thresholds for engineering alloys.

Transition to Steady State

Discussion thus far has pertained to threshold and near-threshold crack growth regime where extrinsic factors, some of them dictated by the microstructural parameters, provide a dominant influence on crack growth rates. With increasing driving force (ΔK) the plastic zone size becomes larger than the controlling microstructural unit to the extent that slip becomes more homogeneous across the grains. This leads to a long uniform crack front with minimum crack tip deflections. The transition from the near-threshold crack growth to steady state (Mode I) crack growth therefore is related to the plastic zone size being larger than the grain size or more specifically the mean slip band obstacle spacing. From Rice's analysis (1974) the cyclic plastic zone size can be represented by

$$L = 0.04 \left(\frac{\Delta K}{\sigma_{cy}}\right)^2 \qquad (24)$$

from which the transition ΔK from near-threshold to steady state growth is given by Yoder and others (1979)

$$\Delta K_{T1} = 5\ \sigma_{cy}\ \sqrt{L} \qquad (25)$$

where σ_{cy} is the cyclic yield stress and L is the average grain size or slip band obstacle size. When grain size of a material is decreased, crack growth rate for a given ΔK changes from structure sensitive (near-threshold behavior) to structure insensitive (steady state behavior). The experimental data for several Ti alloys collected by Yoder and others (1979) is represented in Fig. 10. While eq. 24 provides the grain size at which transition occurs for each ΔK value, the grain size dependence of crack growth rate in the hypo-transition range is represented by Sadananda (1981)

$$\frac{da}{dN} \propto \left(\frac{\Delta K}{B}\right)^{1/2\beta} \left(\frac{1}{L}\right)^{\frac{1-4\beta}{\beta}} \qquad (26)$$

which is based on the dislocation pile up model for faceted mode of crack growth. The material constants B and β are related to the cyclic stress-strain behavior represented by

$$\Delta\sigma = B\ (\Delta\epsilon_p)^{\beta} \qquad (27)$$

If there is no change in the mechanism of crack growth with decrease in ΔK, say from a plastic blunting process to a faceted mode other than increased crack path tortuoisty, then the transition is only apparent in terms of applied ΔK and may vanish if growth rates are represented in terms of effective ΔK. In many alloys however there is transition from non-crystallographic to crystallographic mode of crack growth at least at near-threshold crack growth regimes.

Steady State Crack Growth Rates

Referring to Fig. 1 the dominant fatigue crack growth regime generally refers to the Paris law regime where the da/dN-ΔK curve has the lowest slope with the slope varying from 2 to 4. If crack growth occurs by a plastic blunting process then crack growth rates are related to the crack tip plasticity. In terms of fractographic analysis this mode of crack growth results in ductile striations with spacing between striations equal to crack growth per cycle. The crack growth rates can be related to the crack tip opening displacement and is given by

$$\frac{da}{dN} = \alpha\delta_{CTOD} = \alpha\,\frac{\Delta K^2}{4\sigma_{cy}E} \qquad (28)$$

where α is the geometric factor nearly equal to 0.5. Liu and others (1978) estimated α to be 0.68 using finite element analysis of alternate shear process. Important to note is that the growth rates are inversely proportional to the elastic modulus. This is similar to the dependence of elastic modulus on the intrinsic threshold based on the dislocation

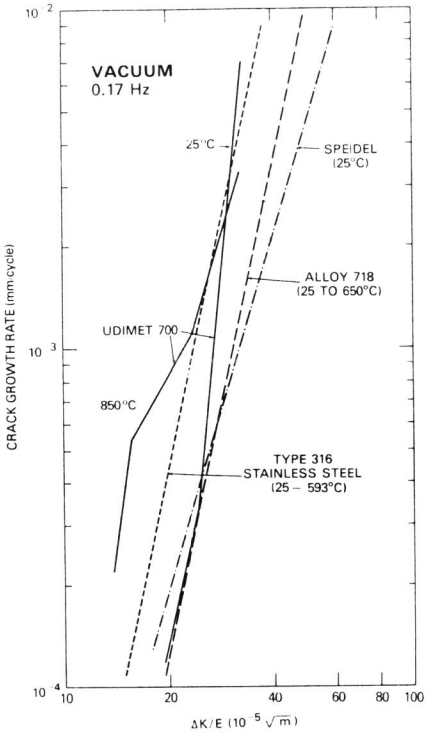

Fig. 11. Normalization of fatigue crack growth data in terms of elastic modulus. Speidel curve corresponds to room temperature behavior of several metals and alloys.

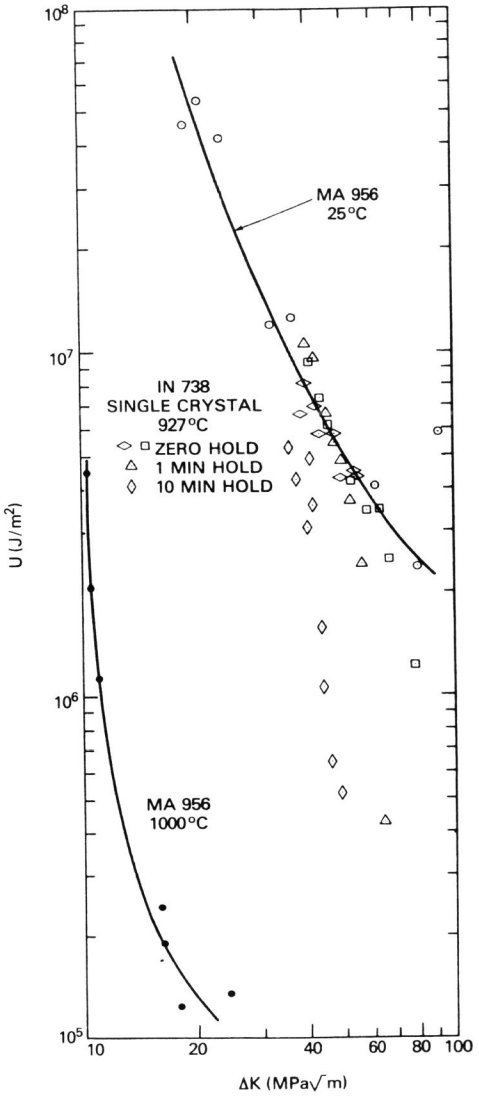

Fig. 12. Variation of hysteresis energy per unit increment in the crack length as a function of the stress intensity range.

nucleation discussed earlier. Speidel (1974) has shown that in the Paris Law regime crack growth rates of many metals can be normalized by their modulus. Fig. 11 shows that crack growth rate variation as a function of temperature in an inert environment for several alloys (Sadananda and Shahinian, 1981a) can also be normalized in terms of elastic modulus provided the mechanism of growth pertains to the plastic blunting process. In the elastic-plastic condition δ_{CTOD} can be represented using the Dugdale crack model as

$$\delta_{CTOD} = \frac{\Delta K^2}{4\sigma_{cy} E} + \frac{A \pi \Delta\varepsilon_p^{(n+1)} a}{2\sigma_{cy}^{(n+1)}} \qquad (29)$$

where n is the cyclic work hardening exponent and a is the crack length. With increasing plasticity the second term dominates to the extent that crack growth rates may not be correlated on the LEFM basis.

When the crack growth process is dictated not by the plastic blunting process but by a cumulative damage process, then eq. 28 is not valid.

The crack growth rates then depend on the nature of the mechanism of the damage. Without knowing the details of the mechanisms involved it is possible to establish crack growth rate - ΔK relation simply on the basis of the energy balance and can be represented by (Weertman, 1978)

$$\frac{da}{dN} = \frac{\Delta K^4}{8\pi^2 \mu \sigma_{cy}^2 U} \qquad (30)$$

where U is the hysteresis energy for a unit increment in the crack length. It is assumed that hysteresis energy is a measure of the irreversible damage ahead of the crack tip and all of this energy is utilized in the fatigue crack growth process and is eventually dissipated as heat with very little stored as internal energy. Equations similar to the above have been derived by Rice (1967), Mura and Lin (1974) and Lindley and McCartney (1981) and their expressions differ from the above by a constant multiplication factor.

Equation 30 appears to provide a fourth power dependence of crack growth rate on ΔK. In reality, however, the hysteresis energy per unit increment in crack length decreases with ΔK and the actual crack growth rate dependence on ΔK can be greater than the apparent fourth power dependence. Figure 12 shows the variation of U with ΔK for several alloys tested in air at various temperatures. Crack growth rates may be predicted using the U values provided cyclic yield stress values are known. Figure 13 shows the predicted growth rates based on eqs. 28 and 30 for an iron base alloy Sadananda (1983) using the values of monotonic yield stress since cyclic yield stress values are not known. The cumulative damage mechanism predicts crack growth rates much better than the plastic blunting process particularly at higher temperature. In fact it was shown that ductile striations were noted only in a limited range of ΔK values at room temperature and still a smaller range at 1000°C. The predicted growth rates based on the cumulative damage mechanisms, eq. 30, and the experimental growth rate curves for a single crystalline turbine blade alloy (Sadananda and Shahinian, 1984) are shown in Fig. 14.

Figures 13 and 14 show that eq. 30 is much more general and relevant to the non-Paris law regime where da/dN varies with ΔK more steeply than given by

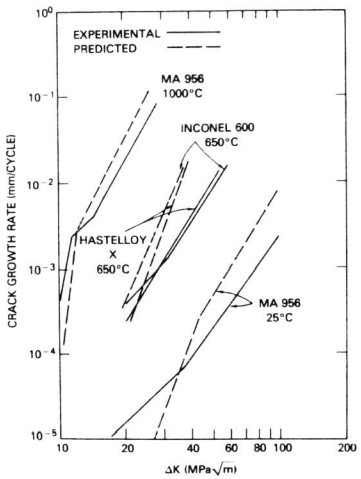

Fig. 13 Comparison of experimental and predicted crack growth rates in several high temperature alloys.

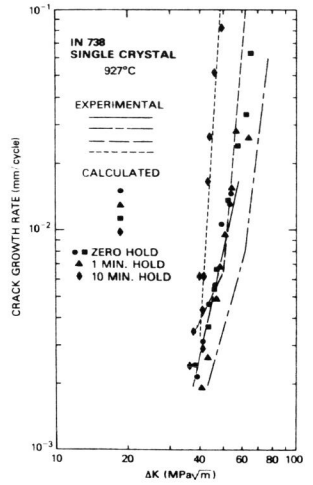

Fig. 14 Comparison of experimental and predicted growth rates in a single crystalline alloy under continuous cycling and cycling with hold times at peak load

the second power relation involving ductile striation mechanisms. That a cumulative damage mechanism predominates in the near-threshold crack growth regime has been discussed earlier. From Figs. 13 and 14 indications are that they are also predominant in the high ΔK end where monotonic fracture processes are superimposed. Here accumulated damage can build up stresses to cause monotonic type of fracture at microstructural heterogeneties ahead of the crack tip accelerating the fatigue crack growth. We note that U values in eq. 30 have been determined experimentally using hysteresis energy measurements. In principle it should be possible to determine U values theoretically on the basis of the micromechanisms that contribute to the cumulative damage. Some of the damage processes have already been discussed with reference to Fig. 3.

Rapid Growth Stage

For completeness we discuss briefly the fatigue crack growth in the final stage of crack growth where da/dN-ΔK curve again becomes steep. That cumulative damage mechanisms operate in this regime is apparent from the above discussion.

Consider that microcracks are forming ahead of the main crack due to monotonic plastic strain that is propagating ahead of the main crack. With the increase in crack length, K_{max} also increases approaching the K_{Ic} the fracture toughness value for Mode I. Even before K_{Ic} is approached there is a finite probability that, at least locally, fracture stresses are attained due to build up stresses. The area fraction of the cracks being formed in this stage can be represented by

$$f = \frac{K_{max}}{K_{Ic}} \qquad (31)$$

The cyclic stress intensity range ΔK will be providing the driving force for the fatigue crack growth process in the remaining area. Because of the reduced area, however, the effective stress intensity at the crack tip is much larger and the proportionate increase in the effective ΔK can be represented by

$$\Delta K_{eff} = \frac{\Delta K}{(1-f)} = \frac{\Delta K}{\left(1 - \frac{K_{max}}{K_{Ic}}\right)} \qquad (32)$$

When K_{max} approaches K_{IC} , f approaches one resulting in rapid increase in the effective ΔK value. Hardrath and others (1978) have recently combined the crack closure concept with superimposed monotonic loading effects to define a new ΔK as

$$\overline{\Delta K} = \frac{\Delta K_{eff}}{\left(1 - \frac{K_{max}}{K_F}\right)} \qquad (33)$$

and have shown that it correlates the crack growth data better than ΔK_{eff} from closure alone. K_F here is equivalent to K_{Ic} but determined under cyclic load conditions.

Recognizing that plasticity effects are becoming increasingly important at high ΔK end, Dowling (1976) evaluated the applicability of J integral under fatigue and showed that the rapid crack growth stage regime extends with the same slope as the Paris law regime when represented in terms of ΔJ. Since ΔJ here is evaluated from the load-displacement loops which takes into consideration the change in the compliance due to superimposed monotonic fracture processes, the ΔJ provides a measure of the effective ΔK at the crack tip. In reality the super-imposed monotonic fracture process contributes to increased crack deflections on one side which reduces the effective ΔK (Fig. 7) and to reduced load bearing area on the other which increases the effective ΔK. The later effect becomes increasingly predominant with increasing crack length to the extent that rapid growth and instability occurs as K_{Ic} is approached.

Short Cracks and Non-propagating Cracks

There appears to be a general consensus that the growth behavior of short cracks is much different from that of long cracks. In particular, crack growth rates are higher and occur at ΔK less than the threshold for long cracks. Crack growth rates are initially high, decrease with increase in ΔK and eventually approach the growth curve for long cracks, depending on the length of the short crack. In some cases the cracks can get arrested completely, resulting in non-propagating cracks. Similar trends in behavior were also noted for the cracks emanating from sharp notches.

Understanding of the short crack growth behavior is important since it provides a link between the crack nucleation stage and the crack propagation stage. The difference in behavior of short cracks from behavior of long cracks arises from several sources. First, in contrast to long cracks, the plastic zone size is comparable to crack size and therefore LEFM is not generally applicable. In addition the crack closure contributions differ

significantly from those of long cracks, further invalidating any similitude. There have been however some attempts to unify the short crack growth behavior with that of long cracks. El Haddad et al. (1979) have defined a fictious length a_o using the endurance limit of a smooth specimen and the linear elastic behavior of the crack, Fig. 15. The data for short cracks fall on the long crack curve if the effective length of the short crack is defined as the actual length plus this fictitious length. In many cases however, a_o is very large and provides an over compensation. Following McEvily (1984), this can be corrected by defining a new a_o^* taking into consideration crack closure effects which reduce the effective ΔK for long cracks. In short, the approaches are only phenomenological and lack physical reasoning. The problem arises from the lack of knowledge of the stress state ahead of a short crack with its associated plasticity. From microstructural considerations, the cracks are of the same size as the microstructural constituents and interaction between the structure and the crack becomes important in controlling the crack growth behavior.

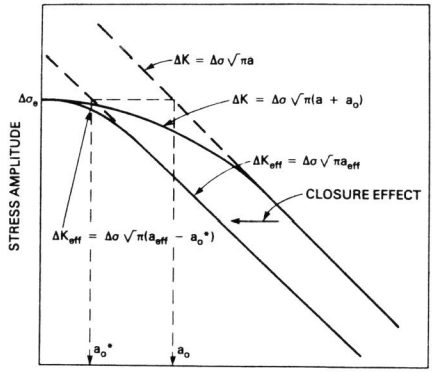

Fig. 15. El Haddad's approach to match short crack growth data with long crack growth data by defining a correction term a_o for crack length. Consideration of crack closure decreases a_o value.

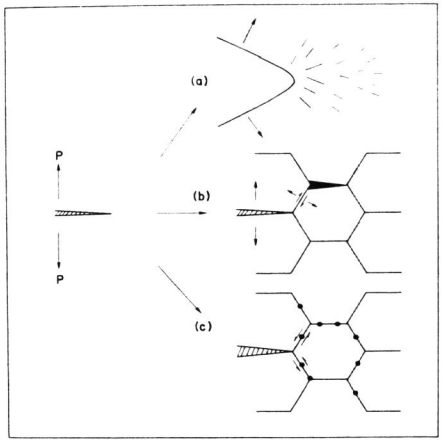

Fig. 16. Schematic illustration showing behavior of cracks under creep load. a) Blunting and formation of fissures ahead of the crack tip, b) grain boundary sliding causing wedge cracks and their growth and c) formation of cavities which grow by plastic deformation.

In summary we have discussed the fatigue crack growth behavior from near-threshold to rapid growth and the micromechanisms involved in each stage. The observed growth rate behavior not only depends on the micromechanisms of the growth but also on the macroscopic growth features in terms of crack path tortuosity and surface roughness. We have not discussed here overload effects where crack closure and crack tip deflection play a role in reducing the effective stress intensity at the crack tip and retarding the growth rates. Likewise the discussion on the effects of

temperature and microstructure has been limited. These aspects, however, have been discussed previously by Sadananda and Shahinian (1981b). In the next few pages we will discuss briefly some of the advances made in understanding creep crack growth behavior. For a more detailed analysis of creep crack growth behavior and theoretical modelling the reader is referred to the recent review by Sadananda and Shahinian (1981c).

CREEP CRACK GROWTH

In contrast to fatigue, creep is a monotonic deformation process and sharp crack tip can be maintained only when the growth can keep pace with the expansion of the creep zone. Creep ahead of the crack tip causes two things. Creep if it is purely homogeneous causes relaxation of crack tip stress fields both by the crack tip blunting process and by the plastic deformation process. In principle creep crack growth can not occur in such a case. The specimen undergoes continuous creep resulting in crack tip blunting, ultimately reducing to a creep rupture type of behavior. In general however creep is nonuniform due to the presence of inhomogeneities such as grain boundaries and precipitates and although stress relaxation occurs due to creep the nonuniformity causes local stress concentrations at triple point junctions and grain boundary precipitates which give rise to nucleation of cavities that grow and coalesce with each other and with the main crack.

Creep may, therefore, be visualized as contributing to two competing processes. Crack tip blunting and creep relaxation of the crack tip stress fields on one side and damage accumulation in terms of cavities and microcracks which grow and coalesce with the main crack and contributes to increase in stresses. The relative rates of stress relaxation rate and damage accumulation rate govern the creep crack growth kinetics. Damage accumulation involves concentration of stresses due to grain boundary sliding and relaxation of these stresses by grain boundary diffusion processes as well as creep deformation. Expressions have been developed for rate of nucleation and growth of cavities due to coupled creep and grain boundary diffusion controlled processes (Beere and Speight, 1978). In principle if the material ahead of the crack tip deforms at a rapid rate then contribution from grain boundary sliding rate can be negligible, resulting in reduced stress concentrations and a reduced damage accumulation rate. On the other hand if the creep rate is very slow, the grain boundary sliding rate is also slow and stress concentrations are rapidly relaxed by the diffusion processes thereby reducing the damage accumulation rate. Creep crack growth is therefore expected only in an intermediate range of strain rates. Similarly the growth occurs in a limited range of temperatures or stresses where stress relaxation processes occur less rapidly than the damage accumulation process. These observations have been confirmed by several experimental results (Sadananda and Shahinian, 1983a). In most of the alloys tested creep crack growth was found only in a limited range of temperatures. In some of the more ductile alloys such as Hastelloy X and Inconel 600, deformation resulted in rapid blunting of the crack tip without any significant crack growth. In some cases stress relaxation also occurs by the formation of fissures around the crack tip resulting in crack arrest. Figure 16 shows schematically the micromechanisms of creep crack growth observed in structural alloys.

Significant work is being directed towards determining the characterizing parameter that can uniquely correlate crack growth rates in an alloy (Sadananda and Shahinian, 1981d). Of the three parameters that have been extensively used, namely stress intensity factor K, elastic-plastic

parameter J^* and reference or equivalent stress σ_r, K is valid only when crack growth occurs rapidly in pace with the growth of the creep zone that lies within the K field, σ_r is valid when creep zone propagates rapidly to the specimen boundaries before any crack growth occurs and J^* is more likely to be applicable when the creep zone is outside the K field but less than specimen boundaries. Riedel and Rice (1980) derived an expression for a characteristic time when the creep zone becomes equal to the K field and is given by

$$t_c = \frac{K^2 (1-\nu^2)}{E(n+1)J^*} \tag{34}$$

If crack growth is observed within this characteristic time, then K is the likely controlling parameter and if no growth is observed within this time J^* is likely to be the parameter.

Creep crack growth behavior of several alloys is represented in terms of J^* in Fig. 17. There is a general trend that if the growth occurs by the same mechanism such as wedge crack nucleation and growth, then the growth rates in terms of J^* fall within a narrow band irrespective of material and temperature. The implication here is that temperature and material dependence are taken into consideration in the J^* value and growth rates are therefore normalized.

Recent results (Sadananda and Shahinian,1983b) on type 316 stainless steel at 593°C, however, showed that extensive spread in the crack growth data can occur in terms of J^* although the data correlate better with J^* than with K or σ_r. It is recognized that J^* is a steady state parameter where stress state of a creep crack is assumed to reach a steady state value before crack growth occurs. The large spread in the data, particularly during the initial growth regime, could be the result of non-steady state conditions. There have been several attempts to use different types of parameters which can provide better correlation of creep crack growth rates. More recently, Reed and others (1983) suggested a T^* integral for correlation of creep crack growth rates. Unlike the J^* which is based on deformation theory of plasticity (non-linear elasticity) the T^* is based on incremental plasticity which is much more realistic in the plastic regime. Efforts will be directed in the future to evaluate the applicability of this integral to creep crack growth. Wilkinson and Vitek (1982) have developed a general analysis for propagation of cracks by cavitation that can be used provided the stress field ahead of the creep crack is known. Under steady state conditions where J^* parameter is applicable the stresses ahead of the crack can be expressed in terms of the J^*. The growth rates can be expressed in terms of

$$\frac{da}{dt} \propto (J^*)^{\alpha\beta} \tag{35}$$

where β may be 1 to 3 for diffusional growth of cavities depending on the shape of cavities, α is related to the stress field and for power law creeping material with $\varepsilon/\varepsilon_o = (\sigma/\sigma_o)^n$, $\alpha = 1/n+1$. From this analysis it is implied that if $\alpha\beta > 1$, the crack growth rate is independent of the number of cavities being nucleated ahead of the crack tip but depends only on the rate of cavity growth. For diffusional growth of cavities, β varies from 1 to 3 and for $\alpha\beta > 1$, n should be 2 or less than 2 depending on β value. Since for most of the structural alloys $n > 3$, the analysis implies that for diffusional growth of cavities, nucleation of cavities has to be considered in analyzing crack growth rates. If cavity growth occurs by creep deformation β may be equal to n and $\alpha\beta \approx n/n+1 \approx 1$ for large n. For this condition both

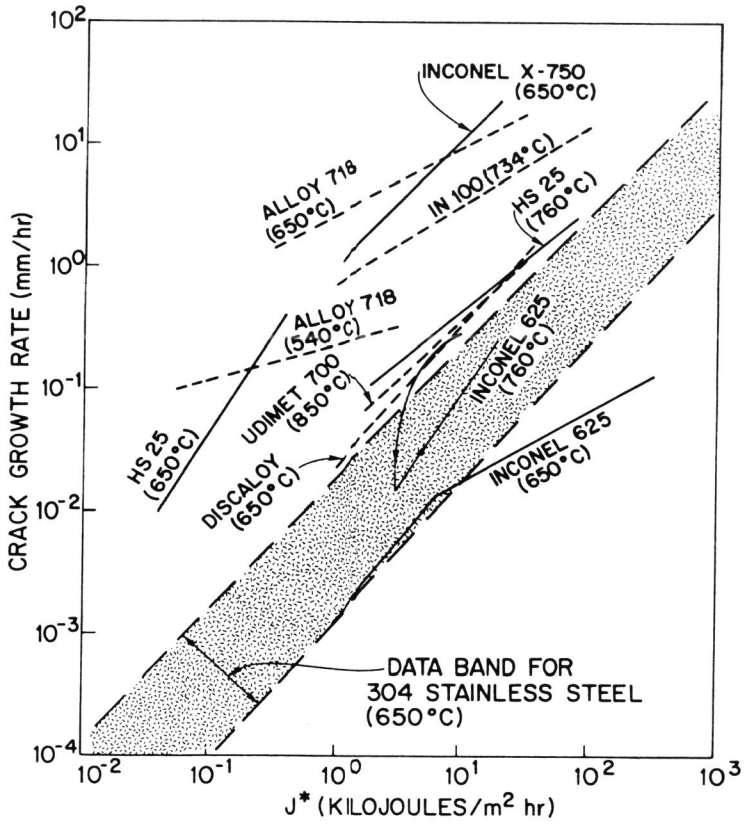

Fig. 17. Creep crack growth rates in several alloys in terms of J^* parameter. Growth rates are higher in alloys that are sensitive to environment.

nucleation and growth rate of cavities may be important for creep crack growth.

While creep crack growth has been studied mostly in polycrystalline materials where crack growth occurs by intergranular fracture, we have studied recently crack growth in cast single crystalline alloys and in mechanically processed oxide dispersion strengthened alloys with high grain aspect ratio. In single crystalline alloys, dendritic boundaries with precipitate network provided the crack path. In a MA 956 alloy, crack growth was also transgranular with oxide dispersoids providing the nucleation centers for cavities. The nucleation and growth of cavities is essentially by the creep deformation process. In fact crack growth in this alloy occurs sufficiently rapidly that creep is much more damaging than fatigue in terms of crack growth rates.

SUMMARY AND CONCLUSIONS

An extensive analysis of fatigue crack growth has been presented in terms of the theoretical understanding of crack growth both from micro-mechanisms and from macromechanics considerations. Threshold, near-threshold crack growth, Paris-law regime and the rapid growth stage have been analyzed. Measured threshold values are affected by the intrinsic factors such as elastic modulus and microstructure and extrinsic factors such as crack closure and crack path tortuosity. Crack growth rates both in the near-threshold regime and in the rapid crack growth regime are governed by the cumulative damage processes where damage is accumulated in each cycle and the crack length increment occurs after several cycles. The nature of the damage could be different in the two regimes. In the Paris-law regime crack growth appears to be predominantly by the plastic blunting process. Effects of crack path tortuosity and crack closure have been discussed in terms of their effect on the da/dN-ΔK curve. Behavior of short cracks and non-propagating cracks have been discussed briefly.

Growth of creep cracks was discussed in terms of the relative kinetics of the stress relaxation processes and the damage accumulation processes. In most of the alloys growth occurs only in a limited range of temperature, stress or strain rate and is related to the fact that only within the specified ranges the damage processes are faster than the stress relaxation processes. Recent developments in the parameteric analysis and in the theoretical modelling of crack growth have been outlined.

ACKNOWLEDGMENTS

It is a pleasure to acknowledge helpful discussions with Drs. P. Shahinian and V. Provenzano of NRL and Dr. S. Suresh of Brown University. Thanks are due to Dr. Shahinian for his critical review of the manuscript. The present research effort was supported by the Office of Naval Research.

REFERENCES

Beere, W. and Speight, M. V., Met. Sci., 12, 1978, 593.
Chakaraborty, S. B., Fatigue of Engrg. Mater. & Struc. 2, 1979, 331.
Davidson, D. L., Fatigue Mechanisms, ASTM STP 675, 1979, 254.
Dowling, N. E., Cracks and Fracture, ASTM STP 601, 1976, 19.
Elber, W., Engrg. Frac. Mech., 2, 1970, 37.
El Haddad, M. H., Smith, K. N. and Topper, T. H., J. Eng. Mater. Tech., Trans. ASME, 101, 1979, 42.
Faber, K. T. and Evans, A. G., Acta Met., 31, 1983, 565.

Gell, M. and Leverant, G. R., Acta Met., 16, 1968, 533.
Gerberich, W. W. and Moody, N. R., Fatigue Mechanisms, ASTM STP 675, 1979, 292.
Hardrath, H. F., Newman, Jr., J. C., Elber, W. and Poe, Jr., C. C., Fracture Mechanics, Perrone, N. et al eds., University of Virginia, Charlottesville, 1978, 347.
Kanninen, M. F. and Atkinson, C., Int. J. Frac., 16, 1980, 53.
Laird, C. "Fatigue Crack Propagation," ASTM STP 415, 1967, 131.
Lin, G. M. and Fine, M. E., Scripta Met., 16, 1982, 1249.
Lindley, T. C. and McCartney, L. N., Developments in Fracture Mechanics, Chell, G. G. ed., Applied Science, London, 1981, 247.
Liu, H. W., Young, C. Y. and Kuo, A. S., Fracture Mechanics, Perrone, N. et al eds., University Press of Virginia, Charlottesville, 1978, 629.
Lucas, J. P. and Gerberich, W. W., Fatigue of Engrg. Mater. & Stru., 6, 1983, 271.
McEvily, A. J., Concepts of Fatigue Crack Growth Thresholds, AIME Symposium, Philadelphia, 1983, In Press.
McEvily, A. J., Concepts of Fatigue Crack Growth Thresholds, AIME Symposium, Philadelphia, 1983, In Press.
Mughrabi, H., Herz, K. and Stark, K., Int. J. Fracture, 17, 1981, 193.
Mura, T. and Lin, C. T., Int. J. Fracture, 10, 1974, 284.
Reed, K. N., Stonesifer, R. B. and Atluri, S. N., Non-linear Constitutive Relations for High Temperature Applications, Proc. Symp., NASA Conf. Pub. 2271, 1983, 305.
Rice, J. R., Fatigue Crack Propagation, ASTM STP 415, 1967, 247.
Rice, J. R., J. Mech. Phys. Solids, 22, 1974, 17.
Riedel, H. and Rice, J. R., Fracture Mechanics, ASTM STP 700, 1980, 112.
Sadananda, K., Dislocation Modelling of Physical Systems, An Acta-Scripta Metallurgica Conference, Ashby et al eds., 1981, p. 69.
Sadananda, K., Scripta Met., 17, 1983, 1419.
Sadananda, K. and Shahinian, P, Int. J. Fracture, 13, 1977, 585.
Sadananda, K. and Shahinian, P., Met. Trans., 12A, 1981, 343.
Sadananda, K. and Shahinian, P., Cavities and Cracks in Creep and Fatigue, Gittus, J. ed., Applied Science, London, 1981b, 109.
Sadananda, K. and Shahinian, P., Metal Sci., 15, 1981c, 425.
Sadananda, K. and Shahinian, P., Engrg. Frac. Mech., 15, 1981d, 327.
Sadananda, K. and Shahinian, P., Met. Trans., 14A, 1983a, 1467.
Sadananda, K. and Shahinian, P., Elastic-Plastic Fracture Mechanics, ASTM STP 803, 1983b, I-690.
Sadananda, K. and Shahinian, P., Unpublished, 1984.
Speidel, M. O., High Temperature Materials in Gas Turbines, Sahm, P. R. and Speidel, M. O. eds., Elsevier, Amsterdam, 1974, 207.
Starke, Jr., E. A., Lin, F. S. and Heikkenen, H. C., Concepts of Fatigue Crack Growth Thresholds, AIME Symposium, Philadelphia, 1983, In Press.
Suresh, S., Met. Trans., 14A, 1983, 2375.
Suresh, S. "Concepts of Fatigue Crack Growth Threshold," -AIME Symposium Philadelphia, 1983 -In Press.
Taylor, G. I., J. Inst. Met. 62, 1938, 307.
Weertman, J., Fatigue and Microstructure, ASM Seminar, American Society for Metals, Ohio, 1978, 279.
Weertman, J., Phil. Mag., 43, 1981, 1103.
Wilkinson, D. S. and Vitek, V., Acta Met. 30, 1982, 1723.
Yoder, G. R., Cooley, L. A. and Crooker, T. W., Met. Trans., 8A, 1977, 1737.
Yoder, G., Cooley, L. A. and Crooker, T. W., J. Engrg. Mater. & Tech., Trans. ASME, 101, 1979, 86.
Yokobori, T., Yokobori Jr., A. T. and Kamei, A., Int. J. Fracture, 11, 1975, 781.